

# Structure of Dense Colloidal Liquids in Tight Spaces<sup>1</sup>

Eric R. WEEKS<sup>2</sup> and Carolyn R. NUGENT<sup>3</sup>

## Summary

We use three-dimensional confocal microscopy to study the structure of a dense colloidal liquid confined between two parallel glass plates. The colloidal sample is at a volume fraction of 50% and is a binary mixture of 2  $\mu\text{m}$  and 3  $\mu\text{m}$  diameter particles to prevent crystallization. The plate separation ranges from 50 small particle diameters to 3 small particle diameters. While particles form layers immediately adjacent to the confining walls, we otherwise see little influence of the confinement on structure.

## 1. Introduction

Phase transitions are usually investigated in the context of macroscopically large systems. However, confining samples so that one or more dimensions are microscopic leads to new physics, including confinement-driven phases [1]. Our interest in this paper relates to amorphous phases: liquids and glasses. In particular, the glass transition temperature  $T_G$  is often changed for a confined material [2].  $T_G$  is defined based on a sharply increasing viscosity, or other standard methods [3, 4]. In some experiments, the glass transition temperature is decreased upon confinement (as compared with the transition temperature in bulk), whereas in others, the glass transition temperature increases [2]. Computer simulations indicate that confinement influences the arrangement of atoms [5, 6, 7, 8], which might in turn relate to the change of the glass transition temperature. However, it is difficult to probe structure in nano-confined materials.

We study confinement effects on a dense colloidal liquid, a model system which has a glass transition. Colloids are comprised of small solid particles in a liquid; often these are thought of as like hard spheres. When the particle concentration becomes sufficiently

high, the sample is analogous to a glass: it is microscopically structurally disordered, yet behaves macroscopically like a solid rather than a liquid [9]. Much previous experimental work has verified a variety of similarities between the colloidal glass transition and glass transitions in molecular systems [10, 11, 12, 13]. In our experiments, we study the structural characteristics of a dense colloidal liquid confined between two quasi-parallel plates, by using laser scanning confocal microscopy to directly image the particles [14]. We use a binary mixture of two particle sizes to prevent crystallization [15], similarly to simulations which often use two particle species [5, 8]. The walls induce layering of particles, but we find that confinement has little other apparent influence on the structure of the sample.

## 2. Experimental Details

We use colloidal poly-methyl-methacrylate (PMMA) particles, sterically stabilized to prevent inter-particle attraction [9, 10, 17]. The particles are in a mixture of cyclohexylbromide and decalin, which matches their index of refraction and density [17]. While the particles are similar to previous ones that act like hard spheres [9], in the solvent mixture we use the particles are slightly charged and thus have a slightly soft repulsive interaction in addition to the hard-sphere core. To prevent crystallization which would otherwise be induced by the walls [15], we use a mixture of two particle sizes, with radii

---

1. Manuscript received on April 23, 2007.  
2. Associate Professor, Department of Physics, Emory University, Atlanta, GA 30322, U.S.A.  
3. Former Undergraduate Researcher, Department of Physics, Emory University, Atlanta, GA 30322, U.S.A. At present: UCLA, Geophysics and Space Physics, Los Angeles, CA, U.S.A.

$a_{\text{small}} = 1.18 \mu\text{m}$  and  $a_{\text{large}} = 1.55 \mu\text{m}$ . The two species are approximately equal volume fractions,  $\phi_{\text{small}} \approx \phi_{\text{large}} \approx 0.25$ , so the total overall volume fraction is  $\phi = 0.50 \pm 0.05$ . The uncertainty of  $\phi$  is due to difficulties in precisely determining the individual species particle size, polydispersity of particle sizes (5% for both species), and difficulties in determining relative volume fractions of the two species. The sample is a colloidal liquid – while the exact glass transition volume fraction is unknown for this particular binary mixture, we estimate it to be  $\phi_g \approx 0.6$ .

The sample is placed in a wedge-shaped sample chamber, as shown in Fig. 1. This chamber is formed by placing a thin piece of mylar plastic on one edge of a microscope slide, and then putting a glass coverslip on the slide so that one end rests on the plastic and the other directly against the slide, similar to the method used by Refs. [15, 16]. The “thin” end directly against the slide is clamped, and the chamber glued shut except for two small holes. The sample is then added through one hole, allowing air to escape through the other hole. The resulting shape is as described in Fig. 1: a very long sample chamber that ranges in thickness. The two plates are not exactly parallel, but are tilted at an angle of  $0.4^\circ$  relative to each other.

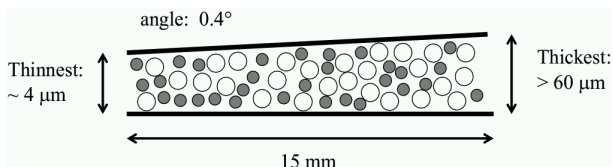


Fig.1 Sketch of sample chamber (not to scale). The small particles are  $2.36 \mu\text{m}$  in diameter and are shaded gray to indicate that they are fluorescently dyed. The large particles are  $3.10 \mu\text{m}$  in diameter and are drawn in white to indicate that they are not dyed and thus invisible to the confocal microscope.

We use laser scanning confocal microscopy to view the sample [14, 17]. This allows us to scan a three-dimensional picture of the sample, with image dimensions  $50 \times 50 \times 20 \mu\text{m}^3$ . We use a fast confocal microscope (the Visitech “VT-Eye”) which can scan this volume in 2.0 s, thus providing a nearly instantaneous snapshot of the sample, assuming particles don’t move much in that amount of time. This condition is easily met in our dense colloidal sample, where particles typically take  $\sim 100$  s to diffuse their own diameter

[18]. The small particle species is dyed with rhodamine dye [17], and the large species is left undyed. Thus in the results that follow, all data are for the small species only.

Over our field of view, the change in thickness due to the slight tilt of the sample chamber is less than  $0.3 \mu\text{m}$ , which is negligible for all but the thinnest regions; thus for our analysis, we treat the plates as parallel. We cannot see any influence of the tilt angle in either structure or dynamics, suggesting that this is a reasonable approximation.

### 3. Results

In practice, we find that some particles stick to the sample chamber walls. This is only a small fraction; typically less than 20% of the wall area is coated with stuck particles. The stuck particles are a mixture of small and large particles. From the sequence of 3D confocal images, we use conventional techniques to track the motion of all of the particles in three dimensions [17, 19]. The stuck particles are easily identified by their lack of motion. Because they are stuck to the walls, they serve as a useful tool for measuring the thickness of the sample chamber locally.

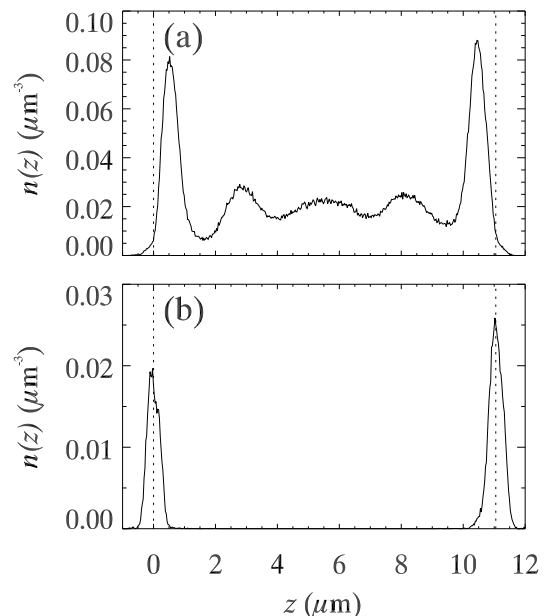


Fig.2 The number density  $n$  as a function of the distance  $z$  between the walls. (a) All mobile particles. (b) All immobile particles. The vertical dotted lines in both panels indicate the mean  $z$  position obtained from the immobile particles of (b). The distance between these two positions gives  $H = 11.05 \mu\text{m}$  for these data.

To determine the chamber thickness, we measure the number density  $n(z)$  as a function of the distance  $z$  between the walls. A typical example is shown in Fig. 2, where (a) shows the free particles and (b) shows the stuck particles. From data such as Fig. 2(b), it is easy to determine the center of each peak. This then is the position of the *centers* of the small particles stuck to the walls, and indicates the maximum possible extent for the *centers* of the free particles to be located. These two positions are indicated by the dotted lines in Fig. 2, and their separation determines  $H$ , the effective local chamber thickness. Recall that only the small particles are viewed with the microscope. Thus, the actual sample chamber thickness is  $H + 2a_{\text{small}} = H + 2.36 \mu\text{m}$ . While the uncertainty in locating particle positions is  $0.1 \mu\text{m}$ , by averaging over tens of stuck particles, we can determine  $H$  to within  $0.01 \mu\text{m}$ . Our uncertainty in the particle size is poorer,  $\pm 0.05 \mu\text{m}$ , thus here we report all thicknesses in terms of  $H$ .

Figure 2(a) shows layering of particles near the wall. This has often been seen in computer simulations [6, 20] and experiments [15]. The position of the layer next to each wall is slightly displaced from contact with the wall; compare the position of the stuck particles in Fig. 2(b) with the layers in (a). This is likely due to a like-charge Coulomb repulsion between the walls and the particles. The layers quickly wash out in the interior of the sample, which we attribute to the binary nature of the sample. The spacing between the interior layers is likely due to a mixture of two factors: sitting next to adjacent layers of either small or large particles, and symmetry in  $z$ . (While we do not have data from the large particles, DIC microscopy shows that they too form layers near the walls, albeit with positions that are shifted due to their size.)

One possibility is that the layers may wash out due to quantization effects. For example, if  $H \approx 2ma_{\text{small}}$  for some integer  $m$ , perhaps we would see sharp layers of the small particles. To investigate this possibility, a variety of concentration profiles are plotted in Fig. 3 at different values of  $H$ . Rather than seeing a quantization effect, it appears that the layer adjacent to each of the walls is always prominent, and the interior layers are always greatly reduced. In fact, for the larger thicknesses shown in Fig. 3, the interior layering is almost negligible. (Another possible quantization condition would come from forming hexagonal layers, with a spacing of  $a_{\text{small}}\sqrt{3}$ . For the profiles

shown in Fig. 3, the values of  $H$  in terms of  $a_{\text{small}}\sqrt{3}$  are 3.4, 3.8, 4.2, 4.6, 4.8, 5.4, and 5.7.)

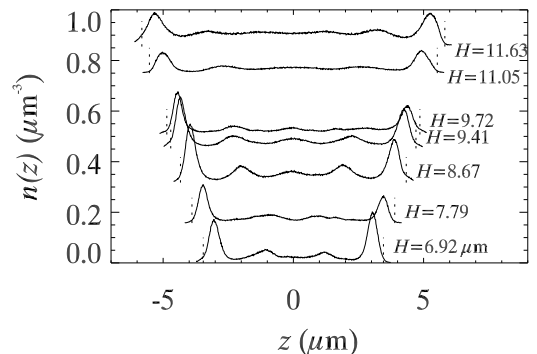


Fig.3 The number density  $n$  as a function of the distance  $z$  between the walls. The curves are centered around the midpoint between the walls, and the thickness  $H$  is as labeled (in microns). The values of  $H$  in terms of  $a_{\text{small}}$  are 5.9, 6.6, 7.3, 8.0, 8.2, 9.4, and 9.9. The curves are vertically offset for clarity, with the offset proportional to  $H$ .

The height of the peaks of  $n(z)$  near the walls changes from sample to sample, although not in a systematic way. This seems to be due to slight variability in the number ratio between big and small particles; more smaller particles results in a higher peak of  $n(z)$ .

One final structural quantity we consider is the pair correlation function,  $g(r)$ . This function relates to the probability of finding a particle a distance  $r$  away from another particle; it is normalized so that  $g(r) = 1$  for  $r \rightarrow \infty$ . Figure 4 shows  $g(r)$  for several different thicknesses  $H$ , for the small particles. The thicker line indicates the result for large  $H$ , and little difference is seen until  $H < 10 \mu\text{m}$ , where the thickness is only a few particle diameters. At that point, the first peak height begins rising, and the minimum at  $r = 3.7 \mu\text{m}$  decreases slightly. The most pronounced difference is seen in the most confined case,  $H = 7.79 \mu\text{m}$ , where the first peak height rises significantly compared to the other curves. These results indicate that the structure remains relatively unchanged until the confinement becomes rather extreme. Despite the presence of the layers seen in Fig. 3, the pair correlation function shows little variation with thickness over a large range of  $H$ .

One other notable feature seen in Fig. 4 is that the position of the first peak of  $g(r)$  does not change until the most confined case. This suggests that the overall sample volume fraction  $\phi$  is unchanged. (For these slightly charged particles, samples with larger  $\phi$  show a first-peak position at smaller values of  $r$ ,

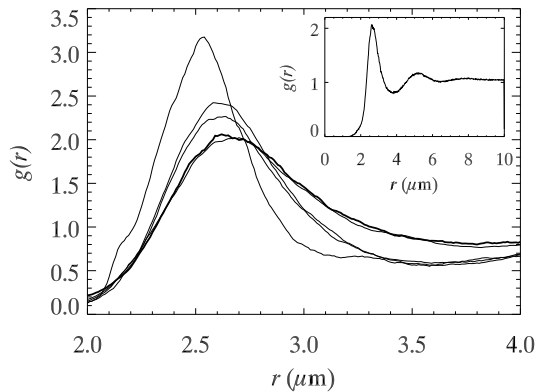


Fig.4 Pair correlation function  $g(r)$  for different thicknesses  $H$ . The solid line corresponds to  $H = \text{bulk}$ , and the peak height increases with decreasing  $H = 16.28, 9.41, 8.67,$  and  $7.79 \mu\text{m}$ . Inset:  $g(r)$  over a larger range in  $r$ , for  $H = \text{bulk}$ .

and this is not seen. For pure hard spheres, the peak position is always at  $r = 2a$ , but this is not the case for our colloids.) The shift in the peak of  $g(r)$  for the thinnest sample ( $H = 7.79 \mu\text{m}$ ) suggests that in that case, the volume fraction may be higher. Of course,  $\phi$  is somewhat poorly defined for samples with such close boundaries, and the change in  $g(r)$  may reflect some other structural configuration present in the thinnest sample.

#### 4. Conclusion

We have studied a dense binary colloidal suspension confined between two nearly parallel plates. While particles form layers immediately adjacent to the plates, the interior of the sample shows much less layering. The pair correlation function changes only slightly, until the point where the distance between the plates is less than  $\sim 4$  small particle diameters (equivalently,  $\sim 3$  large particle diameters). These results seem to indicate that if confinement changes the particle dynamics, as seen in other experiments [2], this is either not due to structural influences, or else the influence of the structure is quite subtle [8]. An alternate explanation might be possible if particle motions only change for thicknesses for which the structure is observed to change; but this seems not to be the case in our experiments. A further study of particle motion is reported elsewhere [18].

#### Acknowledgments

We thank Eric Dufresne, Kazem Edmond, Ming Hsu, and Hetal Patel for useful discussions. We also thank Andrew Schofield and Wilson Poon for providing the colloidal samples. This work was supported by the National Science Foundation under Grant No. DMR-0239109. For correspondence contact ERW: weeks@physics.emory.edu.

#### References

- [1] C. Alba-Simionesco et al.: Effects of Confinement on Freezing and Melting, *J. Phys.: Condens. Matter*, Vol.18 (2006), pp.R15–R68.
- [2] M. Alcoutlabi and G. B. McKenna: Effects of Confinement on Material Behavior at the Nanometre Size Scale, *J. Phys.: Condens. Matter*, Vol.17 (2005), pp.R461–R524.
- [3] C. A. Angell: Formation of Glasses from Liquids and Biopolymers, *Science*, Vol.267 (1995), pp.1924–1935.
- [4] F. H. Stillinger: A Topographic View of Supercooled Liquids and Glass Formation, *Science*, Vol.267 (1995) pp.1935–1939.
- [5] P. Scheidler, W. Kob and K. Binder: The Relaxation Dynamics of a Simple Glass Former Confined in a Pore, *Europhys. Lett.*, Vol.52 (2000), pp.277–283.
- [6] Z. T. Németh and H. Löwen: Freezing and Glass Transition of Hard Spheres in Cavities, *Phys. Rev. E*, Vol.59 (1999), pp.6824–6829.
- [7] P. A. Thompson, G. S. Grest and M. O. Robbins: Phase Transitions and Universal Dynamics in Confined Films, *Phys. Rev. Lett.*, Vol.68 (1992), pp.3448–3451.
- [8] K. Kim and R. Yamamoto: Apparent Finite-Size Effects in the Dynamics of Supercooled Liquids, *Phys. Rev. E*, Vol.61 (2000), pp.R41–R44.
- [9] P. N. Pusey and W. van Meegen: Phase Behaviour of Concentrated Suspensions of nearly Hard Colloidal Spheres, *Nature*, Vol.320 (1986), pp.340–342.
- [10] E. R. Weeks, J. C. Crocker, A. C. Levitt, A. Schofield and D. A. Weitz: Three-Dimensional

- Direct Imaging of Structural Relaxation near the Colloidal Glass Transition, *Science*, Vol.287 (2000), pp.627–631.
- [11] W. K. Kegel and A. van Blaaderen: Direct Observation of Dynamical Heterogeneities in Colloidal Hard-Sphere Suspensions, *Science*, Vol.287 (2000), pp.290–293.
- [12] A. van Blaaderen and P. Wiltzius: Real-Space Structure of Colloidal Hard-Sphere Glasses, *Science*, Vol.270 (1995), pp.1177–1179.
- [13] I. Snook, W. van Megen and P. N. Pusey: Structure of Colloidal Glasses Calculated by the Molecular-Dynamics Method and Measured by Light Scattering, *Phys. Rev. A*, Vol.43 (1991), pp.6900–6907.
- [14] V. Prasad, D. Semwogerere and E. R. Weeks: Confocal Microscopy of Colloids, *J. Phys.: Condens. Matter*, Vol.19 (2007), pp.113102-1–113102-25.
- [15] C. A. Murray: Phases of Thin Colloidal Layers, *MRS Bulletin*, Vol.23 (1998), pp.33–38.
- [16] A. Barreira Fontecha et al.: A Comparative Study on the Phase Behaviour of Highly Charged Colloidal Spheres in a Confining Wedge Geometry, *J. Phys.: Condens. Matter*, Vol.17 (2005), pp.S2779–S2786.
- [17] A. D. Dinsmore, E. R. Weeks, V. Prasad, A. C. Levitt and D. A. Weitz: Three-Dimensional Confocal Microscopy of Colloids, *App. Optics.*, Vol.40 (2001), pp.4152–4159.
- [18] C. R. Nugent, K. V. Edmond, H. N. Patel and E. R. Weeks: Colloidal Glass Transition Observed in Confinement, arXiv:cond-mat/0601648v1 (preprint).
- [19] J. C. Crocker and D. G. Grier: Methods of Digital Video Microscopy for Colloidal Studies, *J. Colloid Interface Sci.*, Vol.179 (1996), pp.298–310.
- [20] A. J. Archer, P. Hopkins and M. Schmidt: Dynamics in Inhomogeneous Liquids and Glasses Via the Test Particle Limit, arXiv:cond-mat/0609663v1 (preprint).